HAL open science

Electroacoustic Resonators: System Identification and Stabililty

Emanuele de Bono, Manuel Collet, Sami Karkar, Gaël Matten, Hervé Lissek, Thomas Laurence

To cite this version:

Emanuele de Bono, Manuel Collet, Sami Karkar, Gaël Matten, Hervé Lissek, et al.. Electroacoustic Resonators: System Identification and Stabililty. 26th International Congress on Sound & Vibration - ICSV26, Jul 2019, Montréal, Canada. hal-02389792

HAL Id: hal-02389792

https://hal.science/hal-02389792v1

Submitted on 31 Oct 2023

HAL is a multi-disciplinary open access archive for the deposit and dissemination of scientific research documents, whether they are published or not. The documents may come from teaching and research institutions in France or abroad, or from public or private research centers.

L'archive ouverte pluridisciplinaire **HAL**, est destinée au dépôt et à la diffusion de documents scientifiques de niveau recherche, publiés ou non, émanant des établissements d'enseignement et de recherche français ou étrangers, des laboratoires publics ou privés.

ELECTROACOUSTIC RESONATORS: SYSTEM IDENTIFICATION AND STABILITY

Emanuele De Bono, Manuel Collet, Sami Karkar
Laboratoire de tribologie et dynamique des systèmes
École Centrale de Lyon, Lyon, France
email: emanuele.de-bono@ec-lyon.fr

Gaël Matten
Univ. Bourgogne Franche-Comté, FEMTO-ST Institute
Department of Applied Mechanics, CNRS/UFC/ENSMM/UTBM, 25000 Besançon, FRANCE
email: gael.matten@femto-st.fr

Hervé Lissek, Thomas Laurence
Laboratoire de traitement des signaux 2
École polytechnique fédérale de Lausanne, Lausanne, Switzerland
email: herve.lissek@epfl.ch

An Electroacoustic Resonator consists of a loudspeaker used as a membrane resonator, through an acoustic pressure-based controlled electrical current, in order to vary its vibrating velocity in response to an exogenous sound field. This way, the loudspeaker membrane can be turned, for example, into an effectively broadband sound absorber. However, the effectiveness and stability conditions of such an active device are intrinsically dependent on the accurate knowledge of its electromechanical constituents and the whole control chain, and any mismatch might impair significantly the control performance. In this paper, we propose a new method for identifying the Thiele-Small parameters of a loudspeaker to be used as an active electroacoustic resonator through a digitally-implemented control architecture. Then, numerical and experimental investigation are undertaken to show how the application of Impedance Control laws affects the stability of the electro-mechano-acoustical system. An experimental verification of the acoustic performance of the proposed control strategy is provided, leading to concluding discussion on further developments.

Keywords: Acoustics, Control, Impedance, Loudspeaker, Stability.

1. Introduction

The electroacoustic absorber concept has been introduced as an effective means of damping the duct modes, either using shunt loudspeaker technique [1], direct feedback control [2], or by self-sensing control of the loudspeaker impedance [3]. Rivet et al. [4] showed that a loudspeaker and a microphone nearby, both being connected by a model-based transfer function, can be used for matching the impedance of a loudspeaker diaphragm to a target specific acoustic impedance, which has the effect of damping the

standing waves in an enclosure. The loudspeaker is controlled through a programmable Digital Signal Processor. The pressure-based, current driven loudspeaker control strategy has been applied in an array of electroacoustic absorbers to produce a liner. Its performances in terms of Insertion Loss have been numerically and experimentally analyzed [5], both without airflow and with low Mach numbers (up to 1.5). Previously, Collet et al. [6] proposed and experimentally analyzed the potential of a *Distributed* Impedance Control law. It differentiates for the impedance is substitued by a differential operator contemplating the variation of pressure along the longitudinal direction of the duct. For this reason, the array of controlled cells realizes a non-locally reacting (or *Distributed*) impedance, whose coupling with the acoustic domain and its *Diode Effect* is analytically and numerically analyzed in [7].
The main interest of the *model-based* Impedance Control techniques through electrouacoustic resonators, relies into the possibility to significantly widen the frequency bandwidth of efficiency respect to the classical liners, as well as to move this range in order to adapt to different operating conditions of the air duct where the liner is applied.
Nevertheless, the performances of the Impedance Control techniques are very highly dependent upon the accuracy of the loudspeaker model, as well as upon the inevitable delay in the application of the numerical control.

2. Thiele-Small parameters indentification of an Active Electro-Acoustic Resonator

The mechanical dynamics linking the loudspeaker velocity v and the local pressure p, the electrical dynamics linking the current i and the voltage u at the loudspeaker terminals are reported in Eqs. (1) and (2) respectively. The parameters we want to estimate are: the mechanical mass M_m, the mechanical resistance R_m, the mechanical compliance C_m, the equivalent piston area S_d and the coupling force factor Bl. R_e and L_e are the electrical resistance and inductance of the voice coil respectively. With s we mean the complex variable ($s = j\omega$).

$$Z_m(s)v(s) = S_d\, p(s) - Bl\; i(s) \tag{1}$$

$$u(s) = (R_e + sL_e)\; i(s) - Bl\; v(s) \tag{2}$$

We will present a method for extracting the Thiele-Small parameters for a Single Degree of Freedom electroacoustic resonator model. The technique is based upon the curve fitting of the measured mechanical mobility transfer function between pressure and velocity, around the first resonant frequency of the loudspeaker where Eqs. (1) and (2) are relevant.
The mobility measurements are obtained through a laser doppler velocimeter and a 1/4 inch Brüel and Kjaer microphone, placed close to the loudspeaker membrane, in an approximately open field.

According to the piston-mode approximation, the curve fitting of the mechanical mobility of the loudspeaker, with Open-Circuited terminals, will return an estimation of the mechanical mass, resistance and compliance divided by the equivalent piston area: $\frac{M_m}{S_d}$, $\frac{R_m}{S_d}$, $\frac{1}{C_m S_d}$, see Fig. 1.

$$Y_m(s)\Big|_{i=0} = \frac{v(s)}{p(s)}\Big|_{i=0} = \frac{s}{s^2\frac{M_m}{S_d} + s\frac{R_m}{S_d} + \frac{1}{S_d C_m}} \tag{3}$$

We need now to estimate the force factor Bl, and the equivalent piston area S_d. This is done by two additional equations.

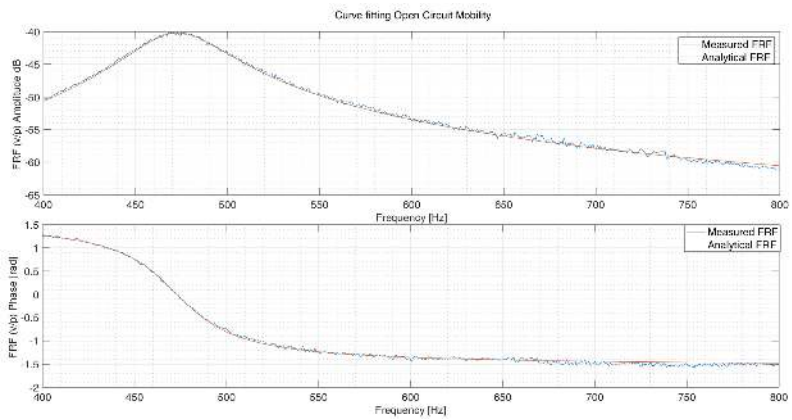

Figure 1: Curve Fitting of the Mobility in case of Open Circuited terminals of the Loudspeaker.

The first one is given by the curve-fitting of the mechanical mobility of the loudspeaker with Short-Circuited terminals. In this case, the voltage will be zero and by neglecting the inductance, we can find a direct proportionality between the current and the mechanical velocity, see Eq. (4).

$$(R_e + sL_e)\, i(s) - Bl\; v(s) = 0 \;\Rightarrow\; i(s) \approx \frac{Bl}{R_e} v(s) \tag{4}$$

By inserting Eq. (4) into the mechanical dynamics Eq. (1), we see that the the short circuit will cause an additional term $(Bl)^2/R_e$ in the mechanical damping, which will reduce the peak amplitude (see Fig. 2). By retrieving the peak amplitude $Q_{S.C.}$ of the mobility measured in the Short Circuited case, we can derive $(Bl)^2/S_d$, with R_m/S_d being already estimated from the curve fitting of the open circuit mobility, see Eq. (5).

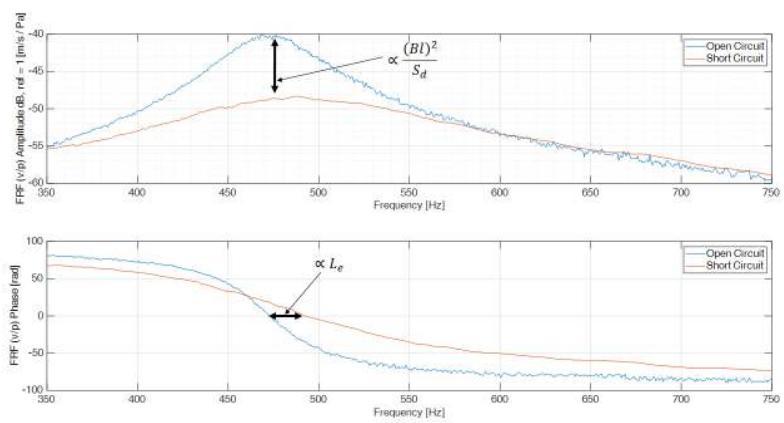

Figure 2: Comparison of Mobilities in case of Open Circuit and Short Circuit terminals. The slight deviation in the resonant frequency in the case of Short Circuit, is due to the neglected inductance.

$$\frac{(Bl)^2}{S_d} \approx (\frac{1}{Q_{S.C.}} - \frac{R_m}{S_d})R_e \tag{5}$$

Another equation can be obtained by applying a current proportional to the pressure ($i = gp$), g being

an arbitrary constant. By doing so, the mobility will traslate upward (for negative small values of g) with respect to the Open Circuit mobility, of a quantity proportional to Bl/Sd (see Fig. 3). If we retrieve the peak amplitude $Q_{P.C.}$ of the measured mobility with the Proportional Control applied, we can finally obtain an expression for Bl/Sd, see Eq. (6). By knowing $(Bl)^2/S_d$ and Bl/S_d, we derive Bl and S_d. Therefore, all the Thiele-Small parameters are finally estimated.

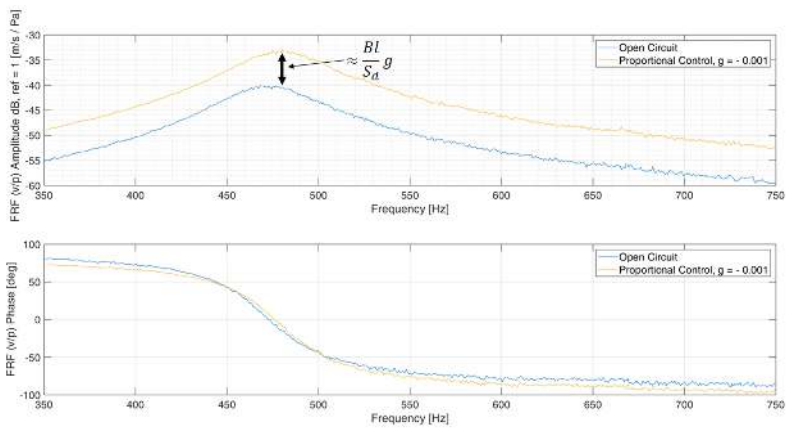

Figure 3: Comparison of Mobilities in case of Open Circuit and Proportional Control.

$$\frac{Bl}{S_d} = \frac{1}{g}(1 - Q_{P.C.}\frac{R_m}{S_d}) \tag{6}$$

Nevertheless, in Eq. (6) we are supposing that the control architecture is capable of reproducing exactly the constant gain between input pressure and output current. We call this method *indirect*, as it does not require the direct measurement of the electrical variables current and voltage, but only of the mechanical mobility, in different configurations. For this reason, it is relatively simple to apply this method to an electroacoustic resonator which can be controlled in current, based upon the measured pressure. On the other hand though, it does not take into account any possible mismatches between the command and the actual injected current in the device, when we are imposing a Proportional Control $i = gp$.

This drawback can be avoided if we access the voltage at the loudspeaker terminals in an open circuit configuration. Indeed, in the open circuit case, the voltage will be directly proportional to the loudspeaker membrane velocity (see Eq. (2)), by the coefficient $-Bl$. The transfer function between velocity and voltage will allow to easily retrieve the force factor. From the knowledge of Bl, and from the estimation of $(Bl)^2/S_d$ obtained in the Short Circuited case (as shown in Eq. (5)), we can get S_d and all the other Thiele-Small parameters.

3. Local Impedance Control strategy

The Local Impedance Control strategy consists of the injection of a current in the loudspeaker coil, which is related to the measured acoustic pressure on the loudspeaker membrane through an appropriate model-based transfer function, capable of reproducing a desired acoustic impedance on the interface with the acoustic medium. This technique is well presented in [4] and the block diagram is reported in Fig. 4.

The corrector H_{loc} and the Target Impedance Z_{at} are reported in Eq. (7). This target impedance was concieved in order to achieve the maximum normal incidence absorption coefficient in a certain

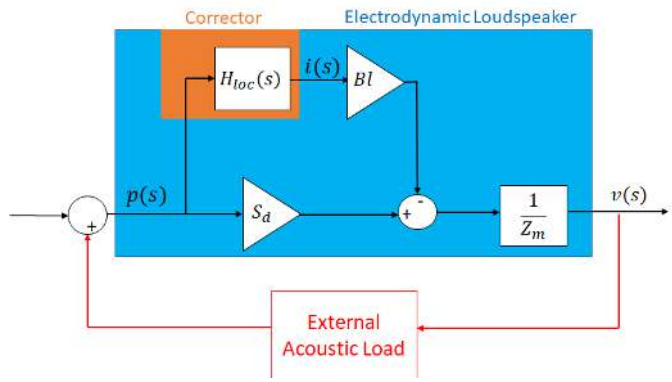

Figure 4: Block DIagram of the Controlled Loudspeaker system.

frequency range. It is therefore a band-pass filter, constituted by a real part which is the target resistance we want to have around the resonant frequency (imposed equal to the air characteristic impedance for getting the maximum normal absorption coefficient), and two additional terms respectively proportional to the mass and compliance of the loudspeaker. These terms are included in order to cut the higher and lower frequency ranges and avoid current saturation. The coefficients μ_1 and μ_2 are responsible for the largeness of the frequency bandwidth of efficient absorption (relative to a threshold value α_{th}), and their ratio determines the resonance angular frequency of the controlled loudspeaker system ω_n, as you can see in Eq. (8). The density and phase velocity of sound in air are indicated by ρ and c_0 respectively, and ω_0 is the natural frequency in rad/s of the loudspeaker without control.

$$H_{loc} = \frac{1}{Bl}(S_d - \frac{Z_m}{Z_{at}}) \quad ; \quad Z_{at} = \mu_1 \frac{M_m}{S_d} s + R_{at} + \frac{\mu_2}{S_d C_m s} \tag{7}$$

$$\Delta\omega\Big|_{\alpha \geq \alpha_{th}} = 2\sqrt{\frac{4R_{at}\rho c_0}{\mu_1^2 M_m^2 \alpha_{th}^2} + \frac{\mu_2}{\mu_1}\omega_0^2} \quad ; \quad \omega_n = \sqrt{\frac{\mu_2}{\mu_1}}\omega_0 \tag{8}$$

As already observed in [4], the block diagram of this pressure-based impedance control technique does not take the form of the typical feedback control architecture, as the feedback between the input variable (pressure) and the output variable (velocity) is realized by the acoustic environment in which the controlled loudspeaker is placed, which varies according to the application. This makes this strategy highly sensitive to incertitudes in the model.

In addition to that, the inevitable time delay in the application of the corrector has the effect of rendering the controlled system, non-minimum phase, i.e. non-passive. Hence, a sufficiently high acoustic feedback will produce instability. The lost of passivity becomes even more critical if coupled with incertitudes in the loudspeaker model parameters.

In Fig. 5 we show the effect of the time delay (τ) on the passivity, by calculating the normal absorption coefficient α of an electroacustic resonator where a Local Impedance Control is applied, with $R_{at} = \rho c_0$, and $\mu_1 = \mu_2 = 0.1$. We can see that as the time delay gets bigger, the passivity condition ($\alpha > 0$) gets broken at lower frequencies, and α reaches more negative values.

As an example of the effect of the model incertitudes on the passivity of the system, in Fig. 6 we compute the impact of an error in the estimation of the mechanical mass of the loudspeaker. We can notice a double significant effect: at resonance frequency, where the absorption coefficient gets lowered and can even become negative, and at the higher frequencies where the absorption coefficient anticipates the break of passivity as the mass parameter gets overestimated.

From these considerations, it comes the necessity of a good estimation of the Thiele-Small parameters adopted in the loudspeaker model, and a way to overcome the break of passivity induced by the time delay.

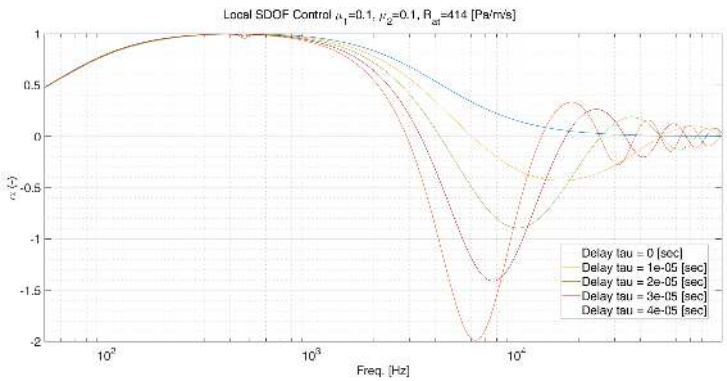

Figure 5: Simulation of the effect of the time delay on the normal Absorption Coefficient of the Local Impedance Controlled loudspeaker.

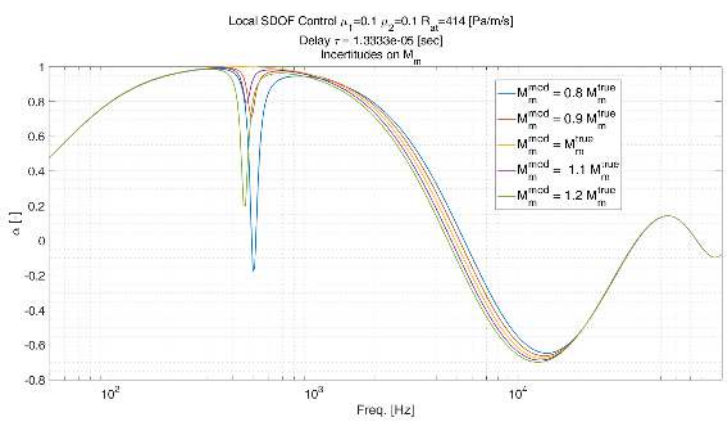

Figure 6: Simulation of the effect of the incertitude in the Mechanical Mass estimation, on the normal Absorption Coefficient of the Local Impedance Controlled loudspeaker.

4. Transmission Loss Performances of Local Impedance Controlled Liner

The Thiele-Small parameters identified through the method described in Section 2 have been used for the model-based corrector transfer function reported in Eq. (7). The controlled cells have been then arranged to create liners to apply on the surface of an acoustic waveguide without flow, and the Transmission Loss is measured.

The Transmission Loss has been evaluated by the transfer matrix method based upon the measurements of pressures upstream and downstream the liner, according to the ASTM E2611-09 standard.
Figure 7 shows the experimental setup used for the evaluation of Transmission Loss. The tube has a squared section of 5 cm side. The duct side is almost coincident with the dimension of the electroacoustic resonator. Each side of the waveguide is lined by a row of six cells, amounting to 24 cells in total. To each cell is applied the Local Impedance Control strategy. In Fig. 8 you can see the measured TLs.

The achievable frequency bandwidth of high transmission loss is limited by the stability. Indeed, the narrowness of our waveguide translates into a high acoustic feedback, which can trigger the instability of the non-passive electroacoustic resonator. In fact, the wider we want to push the frequency bandwidth where the target resistance is obtained, the more *non-passive* each controlled cell becomes. In Fig. 7 the black curve is the TL in the case where the cells are substituted by rigid lids, therefore rendering the duct walls rigid. Nevertheless, we notice some losses due to leakages in the transmission line. The blue curve corresponds to the TL obtained by placing the cells but without controlling them, so that each cell behaves as a passive electroacoustic absorber around its resonant frequency. The violet curve is when the Local Control strategy is applied, using a target resistance $R_{at} = \frac{\rho c_0}{2}$, and $\mu_1 = \mu_2 = 0.4$. In order to furtherly enlarge the frequency bandwidth of efficiency (reducing the μ_1 and μ_2 parameters down to 0.2), a layer of melamine foam of 6 mm thickness, has been placed in front of the loudspeaker membrane, and the curve in red has been obtained. The very thin porous layer has been used in order to cope with the breaking of passivity at the higher frequencies (above 3 kHz), but it does not affect the performances of the cells in the frequency range up to 2 kHz, where the porous layer stays essentilly acoustically transparent. The very high TL achieved (above 40 dB between 500 and 800 Hz, and above 20 dB between 400 and 1000 Hz) in this configuration, reduces the measured pressures downstream the liner to such a point that we cannot retrieve the exact peak value of TL. Compared to the passive resonators-based liners, the frequency bandwidth is much larger, as we have a significant TL up to the double of the natural frequency of the loudspeaker. These results improve also the previous TL performances of the electroacoustic liner presented in [5], thanks to the enlargement of the passivity range obtained through the application of the thin layer of foam.

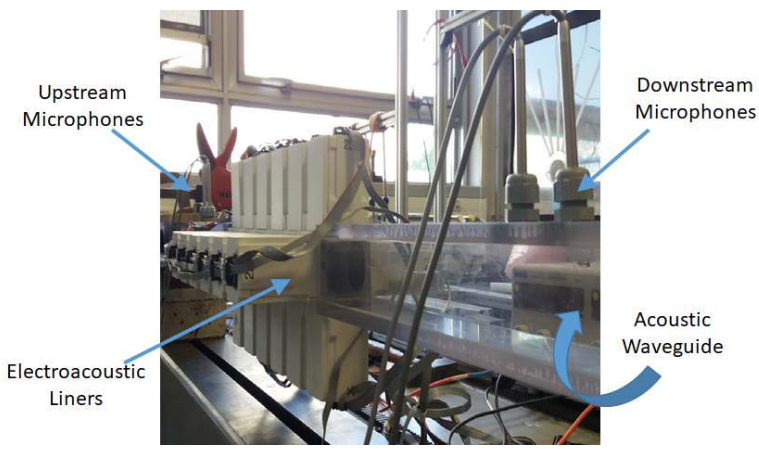

Figure 7: Transmission Loss experimental setup.

4.1 Conclusions

In this contribution, we have proposed an innovative technique to retrieve the Thiele-Small parameters of an electroacoustic resonator. The intrinsical limitations of a current-driven, pressure-based Local Impedance Control require a very good estimation of the model adopted in the corrector transfer function. The inevitable time delay limits the performances of the Impedance Control technique, and its effect is more important if coupled with model incertitudes. Nevertheless, we have experimentally shown the capability of a liner made up of electroacoustic resonators to achieve high values of Transmission Loss in a very large frequency bandwidth. In order to improve the performances of such control technique, it is being synthesized a new corrector through the H_∞ method, which will take into account the robustness

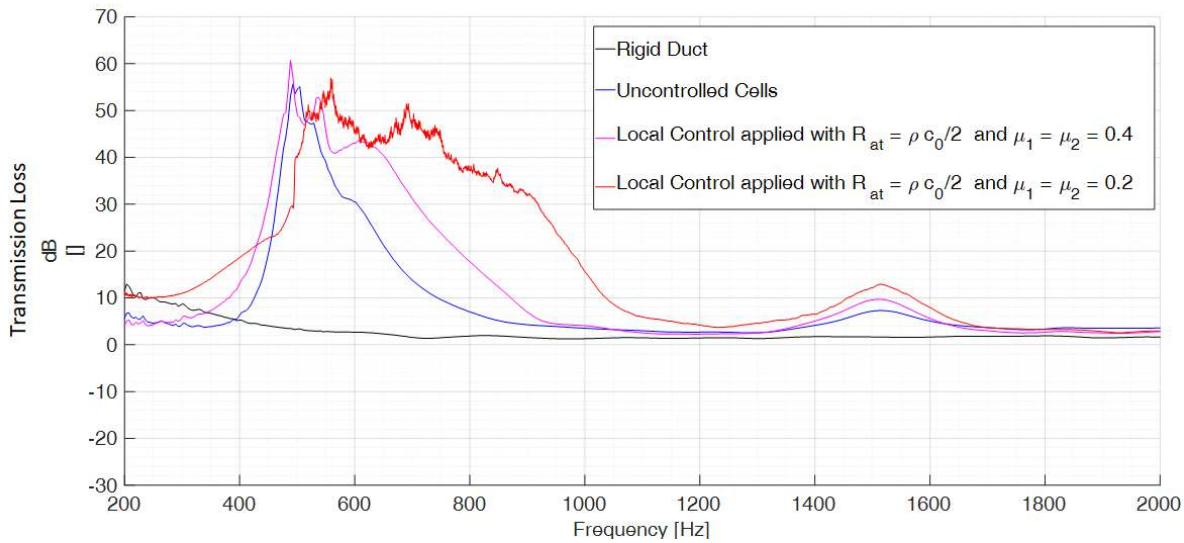

Figure 8: Transmission Loss measurements.

with respect to both performances and stability, since the very early design stage of the corrector.

ACKNOWLEDGEMENTS

This project has received funding from the European Union's Horizon 2020 research and innovation programme under the Marie Sklodowska-Curie grant agreement No 722401.

REFERENCES

1. Lissek, H., Boulandet, R., and Fleury, R., Shunt loudspeaker technique for use as acoustic liner, *Proceedings of the 38th International Congress and Exposition on Noise Control Engineering* 2009, 23-26 August, Ottawa, Canada (2009).

2. Lissek, H., Boulandet, R., and Fleury, R., Electroacoustic absorbers: bridging the gap between shunt loudspeakers and active sound absorption, *Journal of the Acoustical Society of America*, **129** (5), 2968-2978, (2009).

3. Boulandet, R., Rivet, E., Lissek, H., Sensorless electroacoustic absorber through synthesized electrical impedance, *Acta Acustica united with Acustica*, **102**, 696-704, (2016).

4. Rivet, E., Karkar, S., Lissek, H., Broadband low-frequency electroacoustic absorbers through hybrid sensor-/shunt-based impedance control, *IEEE Transactions on Control Systems and Technology*, **25** (1), 63-72, (2017).

5. Boulandet, R., Lissek, H., Karkar, S., Collet, M., Duct modes damping through an adjustable electroacoustic liner under grazing incidence, *Journal of Sound and Vibration*, **426**, 19-33, (2018).

6. Collet, M, David, P., Berthillier, M., Active acoustical impedance using distributed electrodynamical transducers, *The Journal of the Acoustical Society of America*, **125** (2), 882-894, (2009).

7. De Bono, E., Collet, M., Karkar, S., *Analysis of a transport equation as boundary condition in an acoustic transmission line*, ISMA 2018 Conference, Leuven, Belgium, 17–19 September, (2018).